

Regional cerebral glucose metabolism provides a sensitive and specific marker of AD, FTD and MCI, and correlates with CSF Abeta42 level decline in cognitively normal subjects

Dawn Matthews, MS¹, Randolph Andrews, MS¹, Janine Diehl-Schmid, MD², Jordan Grafman, PhD³, Lisa Mosconi, PhD⁴, Mony J de Leon, PhD⁴, and ADNI

¹Abiant, Inc., Grayslake, IL, ²Technische Universität München, Munich, Germany, ³National Institutes of Neurological Disorders and Stroke, Bethesda, MD, ⁴New York University School of Medicine, NY

Background

Measurement of regional cerebral glucose metabolism (rCMglc) using PET imaging has been demonstrated to detect and differentiate Normals (NL), MCI, AD, and frontotemporal dementia (FTD) subjects from multiple academic sites (Mosconi et al, 2008). Improved classification accuracies resulted from incorporation of hippocampal rCMglc measures into the analysis, enabled through a novel automated ROI method (Mosconi et al, 2005; Li et al, 2008). Adoption of PET imaging in the clinical setting requires demonstration across a broad range of sites. Approaches that can resolve the complexity and frequent overlap in regional rCMglc effects of these disease states may further increase accuracy and allow extension to disease subtypes. An understanding of the relationship between rCMglc levels and clinical progression within these heterogeneous categories would add further value. Finally, biomarkers of AD-related amyloid burden and Abeta42 levels have made it possible to explore the temporal relationship between rCMglc changes and pre-symptomatic markers of AD pathology. Together, these advances would enhance the value of PET imaging as an informative, practical diagnostic tool.

Objectives

Our objectives were to:

Measure disease classification accuracies using these methods in a broader population, toward practical clinical application

Evaluate the benefit of combined region of interest (ROI) analysis and a multivariate pattern classification approach

Evaluate the relationship between rCMglc and pre-symptomatic changes in cerebrospinal fluid (CSF) Abeta42 levels

Methods

We analyzed 33 NL, 58 MCI, and 34 AD subjects from the Alzheimer's Disease Neuroimaging Initiative (ADNI) database and 25 subjects diagnosed with frontal/behavioral variant FTD (5 autopsy confirmed) from two additional sites (Technische Universität München, NINDS).

Table 1: Demographic and cognitive characteristics at baseline

Characteristics	NL	MCI	AD	FTD	Total
Number	33	58	34	25	150
Age: Mean (y)	75	75	75	59	72
Range (y)	63-85	55-88	55-86	42-75	42-88
Gender: F	13	20	13	9	55
M	20	38	21	16	95
MMSE	29	27	24		
CDR sum of boxes	0.0	1.7	4.4		

AD subjects were further stratified into AD-VeryMild (baseline CDR=0.5; 14) and AD-MildMod (CDR>0.5; 20). MCI were stratified into MCI-NoDecl (stable ADAS-11 and CDR Sum of Box (SB) scores for 18 months after baseline; 6), MCI-Decl (worsened in ADAS-11 or CDR-SB; 19), and MCI-DeclCon (worsened in ADAS-11 and CDR-SB

or to diagnosis of AD within 24 months; 33). NL were stratified into NL-NL (PIB<1.3 or Abeta42>230, stable ADAS-11 and CDR-SB; 9), NL-LowAB (Abeta42<200, no decline; 18), and NL-Decl (worsened in ADAS-11 or CDR-SB within 18 months after baseline; 6).

All PET scans were processed to uniform resolution as implemented by ADNI (Joshi, 2009) to minimize differences across scanner types.

Automated ROI Method. PET scans were spatially normalized to a custom PET template using a fully reversible transform; this was applied to a set of template ROIs optimized for elderly, neurodegenerative populations, which upon reverse transformation were superimposed onto the subject's native scan to sample without distortion from warping or smoothing of the original image. Univariate and multivariate analyses were performed whereby subjects including completely independent test cases were classified according to Mahalanobis distances from group centroids (Statistica, StatSoft, OK).

Voxel Based Multivariate Analysis. We then applied NPAIRS (Non-parametric, Prediction, Activation, Influence, Re-Sampling) software (Strother et al, 2002; Zheng et al, 2009) to a subset of 24 NL, 24 AD, and 25 FTD subjects. NPAIRS combines a canonical variates (CV) training model with split-half re-sampling to identify the patterns differentiating groups (NL, AD, FTD). Metrics of pattern contribution to total variance, reproducibility, predictive power, subject ranking (CV score(s) and subject influence were produced. New subjects were then scored against classifier CVs.

Results

As shown in Table 2, all classes of subjects showed hypometabolism compared to NL-NL. The extent and magnitude of decline increased in correspondence with severity of clinical decline.

Table 2: Z-scores relative to NL-NL, referenced to pons

Class	HIP	MTL	IPL	PCC	PFC	MFG	OFG	PUT	OCC
NL-NL	0.0	0.0	0.0	0.0	0.0	0.0	0.0	0.0	0.0
NL-LowAB	-1.0	-1.1	-0.8	-0.6	-1.7	-1.1	-1.6	-1.7	-0.1
NL-Decl	-1.6	-1.7	-1.6	-1.5	-2.6	-1.8	-1.9	-2.5	-0.4
MCI-NoDecl	-1.1	-1.2	-1.1	-0.4	-1.9	-1.2	-1.0	-1.5	0.4
MCI-Decl	-2.0	-1.2	-1.2	-0.8	-2.4	-1.6	-1.8	-1.7	0.1
MCI-DeclCon	-3.0	-2.9	-2.2	-1.8	-3.1	-2.1	-2.4	-2.2	-1.1
AD-VeryMild	-2.8	-2.1	-2.8	-1.7	-2.4	-2.0	-2.1	-1.7	0.0
AD-MildMod	-4.3	-3.8	-2.5	-2.0	-3.0	-2.1	-2.4	-2.2	-0.3
FTD	-3.3	-2.7	-2.4	-1.7	-11.2	-5.9	-7.4	-4.8	0.5

Regions shown: Hippocampus (HIP), whole medial temporal lobe (MTL), inferior parietal lobe (IPL), posterior cingulate/precuneus (PCC), prefrontal cortex (PFC), medial frontal gyrus (MFG), orbitofrontal gyrus (OFG), putamen (PUT), occipital lobe (OCC).

Hypometabolism in the FTD group exceeded that of the AD group in prefrontal cortex (p<0.0001), orbitofrontal gyrus (p<0.0001) and putamen (p<0.0001) when referenced to pons.

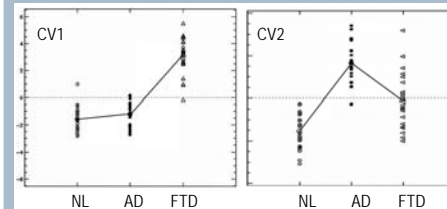
Results of multiple-ROI classification are shown in Table 3 below.

Table 3: Classification Accuracies based upon ROI combinations

Classification	Sensitivity	Specificity	Accuracy
AD vs. NL-NL	97%	100%	98%
FTD vs. NL-NL	96%	100%	97%
FTD vs. AD	100%	97%	98%
MCI-DeclCon vs. NL-NL	95%	100%	96%
NL-LowAB vs. NL-NL	89%	89%	89%

The NPAIRS classification of NL, AD, and FTD yielded 2 canonical variables (Figure 1) and corresponding eigenimages (Figures 2, 3).

Figure 1: Canonical Variates for 3 classes (NL, AD, FTD)



A subject's (circles, triangles) higher placement along the vertical axis indicates greater similarity to the eigenimage pattern relative to subjects at the lower end.

Figure 2: CV1 Eigenimage (representative slices)



Figure 3: CV2 Eigenimage (representative slices)



The first CV accounted for 71% of the variance between the three classes, and separated FTD subjects from NL and AD. The second CV, accounting for 29% of the variance, separated AD from NL. The eigenimage for CV2 exhibits hypometabolism in posterior cingulate/precuneus, parietal lobe, and temporal lobes characteristic of AD. The increase in cerebellum reflects its slower decline relative to global rCMglc in AD, evident due to the use of whole brain as reference for this analysis rather than pons. This difference contributes to the discrimination of disease classes.

Classification accuracy for fifteen blinded NL, AD, and FTD subjects scored against these CV values was 94%. Combining these results with additional ROI information improved accuracy to 100%.

Discussion and Conclusions

The high classification accuracies achieved in our study of subjects from many different imaging sites using multiple scanner types were comparable to the results previously achieved using 7 academic sites (Mosconi et al, 2008).

A progression in the severity of hypometabolism corresponding to sub-classes of clinical progression was demonstrated.

Multivariate analyses applied on an ROI basis and on a voxel basis were instrumental in resolving complex, overlapping patterns. Incorporating ROI measures using our automated method enhanced subject classification by avoiding signal loss from spatial normalization and confirming subjects who deviated from typical group patterns.

Though requiring further study, early Abeta42 changes appear to be associated with initial rCMglc decline.

These results demonstrate the feasibility of achieving high diagnostic accuracies using rCMglc measurement with PET, and provide insight to the temporal emergence of CSF and rCMglc biomarker changes.

References

- Li Y et al (2008) Regional analysis of FDG and PIB-PET images in normal aging, mild cognitive impairment, and Alzheimer's disease. *Eur J Nucl Med Mol Imaging*. 35(12): 2169-81.
- Mosconi L et al (2008) Multicenter standardized 18F-FDG PET diagnosis of mild cognitive impairment, Alzheimer's disease, and other dementias. *J Nucl Med*. Mar;49(3):390-8.
- Mosconi L et al (2005) Reduced hippocampal metabolism in MCI and AD: automated FDG-PET image analysis. *Neurology*. Jun 14;64(11):1860-7.
- Strother SC et al (2002) The quantitative evaluation of functional neuroimaging experiments: the NPAIRS data analysis framework. *Neuroimage*. Apr;15(4):747-71.
- Zhang J et al (2009) Evaluation and optimization of fMRI single-subject processing pipelines with NPAIRS and second-level CVA. *Magn Reson Imaging*. Feb;27(2):264-78.

Acknowledgements and Contact

FTD data was provided by the NINDS and Technische Universität München. Other data used were obtained from the Alzheimer's Disease Neuroimaging Initiative (ADNI) database (www.loni.ucla.edu/ADNI). As such, the investigators within the ADNI contributed to the design and implementation of ADNI and/or provided data but did not participate in analysis or writing of this report. ADNI investigators include (complete listing available at www.loni.ucla.edu/ADNIPublication \ ADNIPublication \ ADNI_Manuscript_Citations.pdf). NPAIRS was developed at the University of Minnesota under the direction of Stephen Strother.

Dawn C. Matthews, Abiant, Inc.
480 West Center Street, Suite 202
Grayslake, Illinois 60030 U.S.A.
Email: dcm@abiant-imaging.com
Website: www.abiant-imaging.com

Tel: 847.707.0370
Email: dcm@abiant-imaging.com
Website: www.abiant-imaging.com